

The Higgs boson at high p_T

Tobias Neumann* and Ciaran Williams†

*Department of Physics, University at Buffalo
The State University of New York, Buffalo 14260 USA*

We present a calculation of $H + j$ at NLO including the effect of a finite top-mass. Where possible we include the complete dependence on m_t . This includes the leading order amplitude, the infrared poles of the two-loop amplitude and the real radiation amplitude. The remaining finite piece of the virtual correction is considered in an asymptotic expansion in m_t , which is accurate to m_t^{-4} . By successively including more m_t -exact pieces, the dependence on the asymptotic series diminishes and we find convergent behavior for $p_T^H > m_t$ for the first time. Our results justify rescaling by the m_t -exact LO cross section to model top-mass effects in EFT results up to p_T of 250 to 300 GeV. We show that the error made by using the LO rescaling becomes comparable to the NNLO scale uncertainty for such large energies. We implement our results into the Monte Carlo code MCFM.

*Electronic address: tobiasne@buffalo.edu

†Electronic address: ciaranwi@buffalo.edu

Contents

1	Introduction	2
2	Calculation	4
2.1	Calculation Details	7
3	Results	7
3.1	Dependence on the asymptotic series	8
3.2	Threshold effects	10
3.3	EFT rescaling approaches	12
3.4	Higgs+jet NLO* phenomenology	16
4	Conclusions	21

1 Introduction

The standout result from the first run of the LHC was the discovery of a Higgs boson [1, 2]. The continued exploration of the physics associated with the Higgs defines one of the key goals of the current run of the machine (Run II). During Run II a much larger data set will be accumulated than that used to initially discover, and study, the Higgs. Accordingly current and future analyses will be able to significantly extend our understanding of the Higgs, and hence the mechanism by which the electroweak symmetry is broken.

Studies of the Higgs boson during Run I were primarily limited to its inclusive properties [3, 4, 5, 6, 7, 8]. Over a range of production and decay channels good agreement ($\sim 10\text{--}20\%$) with the predictions of the Standard Model (SM) was found. With the successful completion of the $N^3\text{LO}$ inclusive Higgs cross section [9, 10] the theoretical errors associated with these measurements should be significantly reduced. In addition to inclusive studies, a major advantage of Run II is the ability to study the Higgs differentially with far greater accuracy than that obtained in Run I [3, 11, 12, 13, 14, 15, 16, 17].

Apart from the intrinsic interest in understanding the only known fundamental scalar, there are strong motivations to understand the Higgs as a tool to discover or constrain Beyond the Standard Model (BSM) physics. The Higgs boson may not be exactly as predicted by the SM: BSM physics could occur, for instance, through extended Higgs sectors (which are possibly in an alignment limit such that the 125 GeV Higgs is SM-like), or through anomalous interactions induced by heavy new particles. The Higgs may couple directly to BSM particles such as top-partners or through portal interactions to scalars associated with additional sectors. Many of these situations are best constrained by investigating the

Higgs at higher transverse energies [18, 19, 20, 21, 22, 23, 24, 25, 26, 27, 28], where the BSM effects can become more apparent than in the inclusive result.

Current precision results for N³LO Higgs inclusive [9, 10], NNLO Higgs plus jet [29, 30, 31, 32] and NLO Higgs plus multi-jets [33, 34, 35] are available in the Effective Field Theory (EFT) limit in which the top quark is integrated out. This is because the technical complexity associated with including the exact top quark loop is significantly greater than for the corresponding calculation in the EFT. For the Higgs inclusive cross section, the exact top mass dependence is known at NLO [36, 37, 38]. Although no exact result is available, the top-mass effects for inclusive Higgs production at NNLO have been computed using an asymptotic expansion [39, 40, 41, 42, 43] and matched to the high energy limit [44, 45, 46, 47]. As a result, the effect of the top-mass was estimated to be at the percentage level on the inclusive cross section. For the Higgs plus one-jet topology currently only LO is known exactly [48, 49]. Additionally, LO predictions are available in the full theory for Higgs plus two [50, 51] and three [52, 53] jets. Combining the various jet topologies with the exact top mass dependence into a matched parton shower framework has also been studied recently [54, 26]. While the analytic calculation of $2 \rightarrow 2$ two-loop amplitudes including the top mass and an external massive boson remains a formidable challenge, exciting recent results using numerical methods to evaluate the two-loop master integrals have been employed to calculate di-Higgs production including the exact top mass at NLO [55, 56]. Finally, top mass effects using the high energy behavior for Higgs plus jet have also recently been studied [57, 58].

We therefore find ourselves in a rather unappealing situation in that, while the EFT works extremely well for inclusive rates and differential predictions at low scales, differential studies which probe scales $\geq m_t$ are exposed to large theoretical uncertainties due to the low perturbative order of the full theory results. To estimate the impact of higher order corrections in the full theory, an asymptotic series in m_t^{-2} was computed [59, 60]. For Higgs transverse momenta p_T up to scales $\simeq m_t$ finite top mass effects could be estimated to be at the few percent level. However, in the region of larger p_T , which we are primarily interested in here, the series rapidly diverged. The principal aim of this paper is to significantly extend the range of validity of the asymptotic series approach, allowing for finite top-mass predictions and more general statements regarding the top mass effects to be inferred. This can be achieved by using, where possible, the full top-mass dependent amplitudes. Given that the process is at NLO, the infrared (IR) poles of the two-loop amplitude (and associated finite pieces) are already known. We will therefore minimize the dependence on the asymptotic series by only using it to compute the finite part of the two-loop virtual amplitude. Our results will be made available in the Monte Carlo code MCFM [61, 62, 63].

Our paper proceeds as follows: In section 2 we discuss the setup of our calculation and

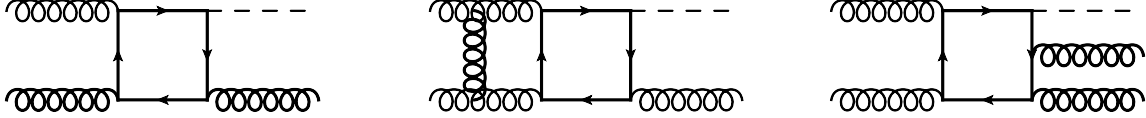


Figure 1: Representative Feynman diagrams for the production of a Higgs boson plus one jet at LO (left) and NLO (center, right). The NLO corrections include two-loop “virtual” topologies (center), and one-loop Higgs plus two parton “real” topologies (right).

detail the exact dependence on the asymptotic series. In section 3 we present our results and compare them to various approximations currently used in the literature. Finally, in section 4 we present our conclusions.

2 Calculation

In this section we discuss the technical details of our calculation and introduce different approximations that have been used to model finite top-mass effects. For illustrative purposes, we show representative Feynman diagrams for the process under consideration in fig. 1. Including the effect of the top-mass in the full theory, the LO calculation corresponds to that of a one-loop amplitude. Given the relative simplicity of this calculation, results have been known for some time [49] (see also refs. [64, 65] for a modern discussion, from which we take the LO amplitudes and tensor structures [64, 66]). The NLO corrections to this process, represented by diagrams such as those in the center and right hand side of fig. 1, are considerably more complicated. The real corrections mandate the inclusion of the Higgs plus four parton amplitudes. This calculation was first performed in ref. [50, 51], studying the top mass effects on Higgs plus two jet production. For the NLO calculation, the presence of the second parton as a jet is not required, and the single unresolved limit of this amplitude is readily explored. Therefore, the computation of this amplitude requires care to ensure numerical stability.

The two-loop virtual corrections, illustrated in the center of the figure, are the most technically challenging part of the calculation. Techniques required to reduce the system to master integrals which can be analytically solved are not yet mature enough to handle tasks of this complexity. However, recent progress using numerical methods to evaluate similar master integrals for di-Higgs productions have recently produced phenomenologically usable results [55, 56]. On the analytic side an analytic NLO calculation of $H \rightarrow Z\gamma$ also marks some progress [67].

Since our calculation is performed at NLO, we can write the two-loop amplitude as

$$\mathcal{A}_j^{(2)}(m_t, m_H, s, t, u) = \mathcal{I}_1^j(\epsilon, s, t, u) \mathcal{A}_j^{(1)}(m_t, m_H, s, t, u) + \mathcal{F}_j^{in}(m_t, m_H, s, t, u). \quad (1)$$

In the above equation s , t and u are the Mandelstam variables associated with the partonic kinematics, m_t and m_H are the masses of the top quark and Higgs boson, respectively. The partonic structure of the amplitude is defined by j , where $j = g$ refers to the $gggH$ amplitude and $j = q$ to $q\bar{q}gH$. In terms of these quantities the above equation states that the two-loop virtual amplitude can be written as a function $\mathcal{I}_1^j(\epsilon, s, t, u)$ which multiplies the one-loop amplitude and a second function $\mathcal{F}_j^{in}(m_t, m_H, s, t, u)$ defining the remaining pieces. Crucially, all the IR poles are contained in the \mathcal{I}_1 piece, such that \mathcal{F}_j^{in} is finite. This IR divergent piece can be obtained from the general structure of QCD amplitudes, [68]. Therefore, the unknown part of the two-loop virtual amplitude corresponds to the \mathcal{F}_j^{in} term.

Given that \mathcal{F}_j^{in} is currently unknown, it is worth discussing the various approximations one could employ to attempt to quantify the effect of the top quark mass. Since the EFT results are known to an impressive NNLO accuracy, a natural thing to do is to use the EFT result rescaled by the ratio of the LO full theory result to the LO EFT result, that is

$$\sigma_{\text{EFT-rescaled}}^{\text{NNLO}} = \sigma_{\text{EFT}}^{\text{NNLO}} \times \frac{\sigma_{\text{FT}}^{\text{LO}}}{\sigma_{\text{EFT}}^{\text{LO}}}. \quad (2)$$

This rescaling will always work at the level of the total cross section, but complications arise when more differential quantities are considered. In general it is not possible to perform this rescaling fully-differentially, since a higher order phase space in the EFT requires a mapping back to the Born phase space of the rescaling. However, after completing the calculation one can rescale an observable by the ratio

$$\frac{d\sigma_{\text{EFT-rescaled}}^{\text{NNLO}}}{d\mathcal{O}} = \frac{d\sigma_{\text{EFT}}^{\text{NNLO}}}{d\mathcal{O}} \times \frac{(d\sigma_{\text{FT}}^{\text{LO}}/d\mathcal{O})}{(d\sigma_{\text{EFT}}^{\text{LO}}/d\mathcal{O})}. \quad (3)$$

This allows one, for instance, to obtain top mass improved p_T^H or y_H distributions. Such an approach was pursued recently [69]. This methodology has two potential drawbacks: Firstly, the ratio may not be defined over the full range of the observable phase space. For example if a jet is required in the final state, the region $p_T^H < p_T^{\text{jet}}$ is non-existent at LO. Therefore, in this region no rescaling can be defined, and a discontinuity in the observable definition is introduced at the phase space boundary. Secondly, the precision of the NNLO calculation is impressive, and one may naturally worry that the LO nature of the rescaling introduces a comparable uncertainty given its low order in the perturbative expansion.

Therefore, a much more appealing rescaling would be

$$\frac{d\sigma_{\text{EFT-rescaled}}^{\text{NNLO}}}{d\mathcal{O}} = \frac{d\sigma_{\text{EFT}}^{\text{NNLO}}}{d\mathcal{O}} \times \frac{(d\sigma_{\text{FT}}^{\text{NLO}}/d\mathcal{O})}{(d\sigma_{\text{EFT}}^{\text{NLO}}/d\mathcal{O})}. \quad (4)$$

The study of this modified rescaling, and its comparison to the equivalent LO definition is a principal aim of this paper.

Aside from rescaling the EFT, one could attempt to compute the top mass effects as accurately as possible with existing tools. At high p_T^H , one expects contributions from $H + 2j$ to be significant. This piece can be computed exactly in the top mass and, therefore, one can set up a calculation which includes these contributions: they constitute the real part of the calculation, such that only the virtual part needs to be approximated. Clearly in order to have a sensible prediction all poles must cancel. This can be done for instance by rescaling the virtual pieces, by the LO ratio. Since the virtual and LO part share the same phase space, this can be performed pointwise. After rescaling, the IR poles cancel and one effectively defines

$$\mathcal{F}_j^{\text{in}}(m_t, m_H, s, t, u) = \mathcal{F}_{j,\text{EFT}}^{\text{in}}(m_H, s, t, u) \frac{\mathcal{A}_j^{(1)}(m_t, m_H, s, t, u)}{\mathcal{A}_{j,\text{EFT}}^{(1)}(m_H, s, t, u)}. \quad (5)$$

Such an approach was undertaken in ref. [54].

An alternative approach to rescaling is to attempt to quantify the top mass effects in $\mathcal{F}_j^{\text{in}}$ approximately with an asymptotic series expansion [70, 71] in Λ/m_t , where Λ can be any kinematical scale of the process. This approach has the advantage that it quantifies the impact of the top mass directly at NLO, but suffers from the disadvantage that such series typically diverge at energy scales Λ comparable to the top quark mass m_t . In this approach one has some freedom in whether the amplitude or the matrix element gets expanded asymptotically. Specifically we define two terms,

$$\mathcal{F}_{j,\text{RI}}^{\text{in}} = 2 \left[\text{Re} \left(\mathcal{F}_j^{\text{in}}(m_t, m_H, s, t, u) \mathcal{A}_j^{(1)}(m_t, m_H, s, t, u)^* \right) \right]_{\text{asy}} \quad (6)$$

and

$$\mathcal{F}_{j,\text{SI}}^{\text{in}} = 2 \text{Re} \left(\left[\mathcal{F}_j^{\text{in}}(m_t, m_H, s, t, u) \right]_{\text{asy}} \mathcal{A}_j^{(1)}(m_t, m_H, s, t, u)^* \right). \quad (7)$$

In the above equations, $[]_{\text{asy}}$ refers to the terms which are asymptotically expanded. In the RI term the full interference is asymptotically expanded, whereas in the SI term only the IR finite parts of the two-loop amplitude are asymptotically expanded.

2.1 Calculation Details

The necessary ingredients for our calculation can be split into two groups corresponding to the real and virtual parts of the calculation. We calculated the Higgs plus four parton loop amplitudes which fully include the effect of the top quark using unitarity techniques outlined in refs. [72, 73]¹. To validate our analytical calculation, we compared it to results obtained using an in-house implementation of the D -dimensional unitarity algorithm presented in ref. [75].

The asymptotic expansion [76, 70, 71] of the two-loop virtual corrections has been performed with the `exp/q2e` [77, 78, 79] codes: the massive one- and two-loop tadpoles were computed with MATAD [79] and massless one-loop integrals were reduced to scalar master integrals with Reduze [80]². To extract the finite piece from the asymptotically expanded result, we subtract the relevant asymptotic expansion of $\mathcal{I}_1^j(\epsilon, s, t, u) \mathcal{A}_j^{(1)}(m_t, m_H, s, t, u)$. The IR poles are then restored in the full theory by replacing these terms with their exact counterparts.

The IR singularities associated with the real and virtual pieces are regularized using Catani-Seymour dipole subtraction [68]. Both the integrated dipoles and real subtraction pieces are defined with the full top mass dependence. The massive scalar master integrals, needed for the evaluation of the matrix elements, are computed with QCDLoop [81, 82]. All parts are assembled in the MCFM framework. For singular regions in the real emission we dynamically switch between double and quad precision.

3 Results

The principal aims of our study are to significantly extend the range of validity of the asymptotic series approach, allowing for finite top-mass predictions, and to investigate the validity of using born rescaling schemes as indicated in section 2. In the first subsection we compare our improved predictions to the full asymptotic series as previously calculated in the literature. The foundation of our study is based on Higgs p_T distributions, where the Higgs can be produced either inclusively or with associated jet requirements. Concerns regarding missing threshold effects in the asymptotic series are also addressed. Subsequently we introduce different EFT rescaling approaches taken in the literature and evaluate their validity. Finally we present some Higgs+jet phenomenology using our recommended predictions.

¹We used the spinor helicity library S@M [74] frequently.

²We would like to thank Tom Zirke for gluing code between `exp/q2e` and Reduze.

Our input parameters are $m_H = 125$ GeV for the Higgs boson mass, $m_t = 173.5$ GeV for the on-shell top-quark mass, and $\mu_R = \mu_F = \sqrt{m_H^2 + p_{T,H}^2}$ for a common renormalization and factorization scale. We use CT14 PDFs [83] at NLO accuracy for the NLO cross sections and at LO accuracy for the LO cross sections. Except for the Higgs inclusive cross sections, and unless specified otherwise, we use the anti- k_T jet algorithm with $p_{t,\text{jet}}^{\text{min}} = 30$ GeV, $|\eta_{\text{jet}}^{\text{max}}| = 5$ and $R = 0.5$.

In order to be as conservative as possible we use a center of mass energy \sqrt{s} of 14 TeV which we consider to be the worst case scenario with respect to finite top-mass effects for the asymptotic series. This is because the expansion is effectively in Λ/m_t , and the kinematical scales Λ grow with \sqrt{s} . Further, the type of experimental analysis which will be particularly sensitive to the high p_T^H region will require a large amount of data. Such a large data set is most likely to be accumulated during prolonged runs at the maximal design energy of 14 TeV.

3.1 Dependence on the asymptotic series

Our first results, for the inclusive Higgs p_T spectrum, are presented in fig. 2. Since the predictions are inclusive, no jet requirement is imposed, we simply require a Higgs boson with $p_T^H \geq 30$ GeV. Shown in fig. 2 are three successive predictions which treat the correction in different approximations. From left to right the number of terms which are asymptotically expanded diminishes. In the leftmost panel the calculation is fully in the asymptotic series (and corresponds to a re-calculation of the existing literature result [59, 60]). The dependence on the asymptotic series is readily apparent. The m_t^{-2} and m_t^{-4} predictions rapidly diverge from each other, indicating poor convergence in the asymptotic series and an inability to accurately quantify the impact of the top mass.

The second (central) plot in fig. 2 displays the (new) prediction obtained with the real pieces computed exactly in the top mass, and the virtual pieces computed in the RI formalism described in section 2, which we recall corresponds to the full interference being asymptotically expanded. It is immediately clear that, when compared to the full asymptotic expansion discussed previously, the dependence on the order in the asymptotic expansion is dramatically reduced. An additional pleasing feature apparent in this plot is made clear upon inspection of the lower panel, which presents the ratio of the m_t^{-2} and m_t^{-4} series to the m_t^0 term. This ratio, in essence, determines the impact of the next order in the asymptotic expansion. At low p_T^H the correction going from m_t^0 to m_t^{-2} is around a few percent. However, the inclusion of the next term in the asymptotic expansion does not significantly change the result in the region $p_T^H < 100$ GeV. Beyond this scale the predictions again begin to differ significantly from one another. However, we postulate that in the region $p_T^H < 100$ GeV the closeness of the two curves indicates a converging

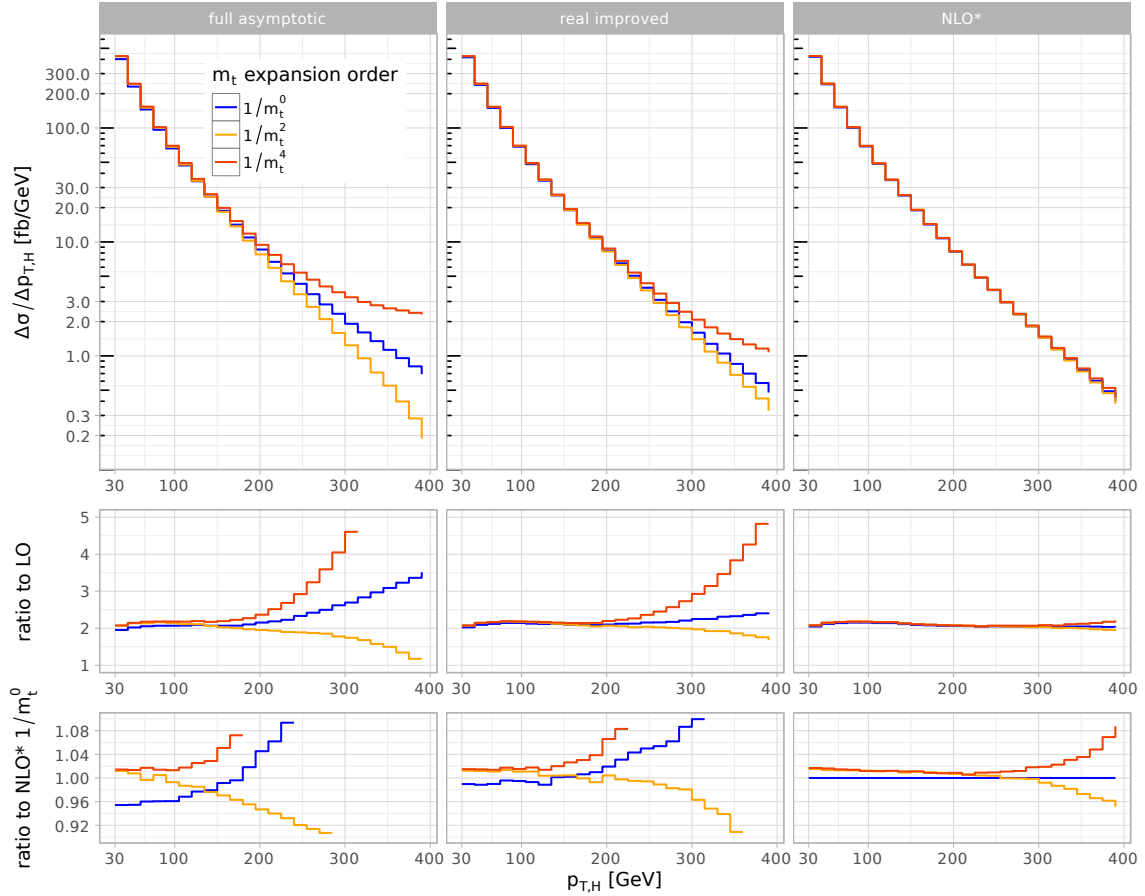


Figure 2: Higgs inclusive p_T spectrum for three different approximations, each taking into account higher orders of an asymptotic expansion in $1/m_t$. The upper panel shows the absolute distribution, while the lower two panels display the ratio to the LO distribution and the NLO* $1/m_t^0$ approximation, respectively.

asymptotic series, and thus deviations from the exact top mass prediction should be essentially zero. A potential fly in the ointment arises from threshold effects, which are not modeled by the asymptotic series. We will address this issue shortly, but for now we use the smallness of the difference between the m_t^{-2} and m_t^{-4} terms to define a region of convergence. Inside this region we postulate that our prediction will accurately capture the top mass effects. For the RI prediction in the central panel, this corresponds to $p_T^H < 100$ GeV.

The final (right) panel in fig. 2 presents the *SI* prediction defined in section 2. For this prediction, only the amplitude for the finite part of the two-loop virtual is obtained in the asymptotic series. The improvement from the central panel is clear, the differences between the m_t^{-2} and m_t^{-4} are even smaller. The region of convergence is significantly extended from around 125 GeV for the RI prediction to around 250 GeV. Crucially, this is the first prediction which extends the region of convergence beyond $p_T^H > m_t$ GeV. We therefore have obtained a prediction which captures the top mass corrections in a stable way beyond the scale in which the EFT breaks down. This prediction therefore represents our best prediction in terms of the small dependence of the order of the asymptotic series. Even in the largest bin the dependence is around 8%, which is still smaller than the NLO scale variation (around 20% which we study shortly). Going forward, we refer to this prediction as NLO*.

3.2 Threshold effects

As briefly mentioned in the previous section, there could be non-negligible threshold effects that are not described by the asymptotic expansion in the convergent region. To address this issue we study the invariant mass spectrum of the Higgs plus hardest jet system $\Delta\sigma/\Delta m_{H,j}$.³ This distribution is shown in fig. 3 at LO. Since the threshold effects are rather small, they are not visible in the absolute distribution in the upper panel of the figure. Instead one has to look at the ratio to the EFT, which contains no finite top-mass effects at all, and thus no threshold effects. In this way any threshold effect will be visible as an increased cross section at $m_{H,j} \simeq 2m_t$. As evident from the plot, the asymptotic expansion correctly converges to the m_t -exact result up to the threshold region beginning at ~ 300 GeV. The one-loop box diagrams lead to a clean threshold effect.

At NLO we take into account the full top-mass dependence of the born piece, the real radiation and all infrared associated pieces of the virtual corrections, as well as the born part of the virtual corrections. The only part where threshold effects are missing are the finite parts of the two-loop integrals entering the virtual corrections, since they are taken

³As a reminder, we use the anti- k_T jet algorithm with $p_{t,\text{jet}}^{\text{min}} = 30$ GeV, $|\eta_{\text{jet}}^{\text{max}}| = 5$ and $R = 0.5$.

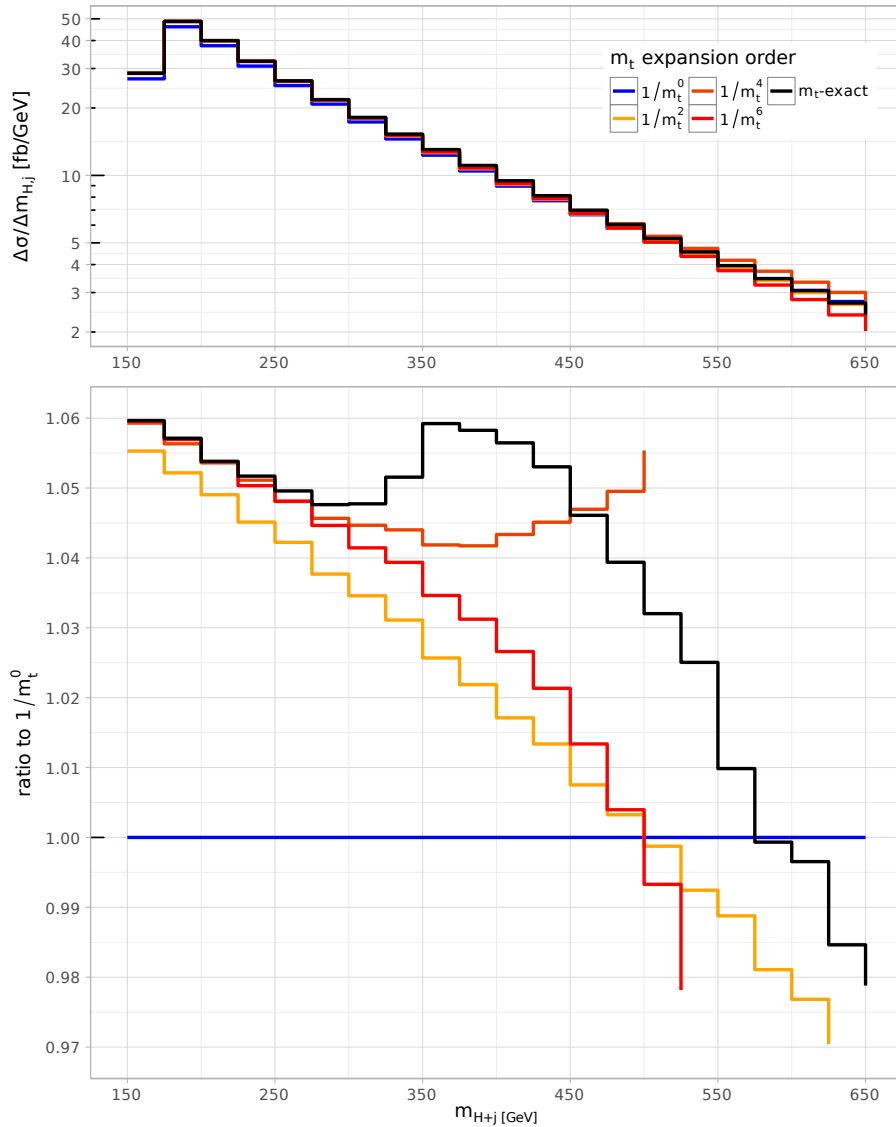


Figure 3: Invariant mass spectrum of the Higgs plus hardest jet system at LO. The upper part displays the absolute distribution, while the lower part displays the ratio to the EFT result.

in the asymptotic expansion.

We show the $\text{NLO}^* \Delta\sigma/\Delta m_{H,j}$ distribution in fig. 4. Again, in terms of the absolute distribution, as shown in the upper panel, the threshold effects are too small to be visible. Therefore, we consider the ratio to the EFT result in the lower panel. With solid lines we show our NLO^* results, whereas with dashed lines the results of the full asymptotic expansion are displayed. The green dashed curve shows the LO/LO-EFT rescaled NLO-EFT result. Since latter is used as a normalization, the green dashed curve in the lower panel coincides with the m_t -exact black curve in the lower panel of fig. 3.

Firstly, let us note that we see convergence of the asymptotic series for our NLO^* result over the whole mass range considered. As expected, since we take into account all those m_t -exact pieces as stated previously, we see an enhancement in the region of $\simeq 350$ GeV. It is also evident that the full asymptotic expansion does not model the threshold effects at all. Our improved result however does show features of a threshold. This alone does not allow us to draw conclusions about the threshold effects we miss through the finite piece of the two-loop integrals, but the comparison with the LO rescaled EFT result does: The LO rescaled EFT result shows threshold effects of a similar magnitude and shape. We also note that the real radiation has a significant impact on the observable, softening the spectrum. In summary, we are satisfied that we capture the dominant threshold effects and that any deviations induced by the missing finite two-loop virtual amplitude should be minor.

3.3 EFT rescaling approaches

In this subsection we compare various EFT rescaling approaches to our improved NLO^* results. We investigate the difference with respect to an overall rescaling of the virtual EFT piece as outlined in eq. (5) (for notational convenience we refer to this as NLO^\dagger) and consider the ratios $\text{NLO}^*/\text{NLO-EFT}$, $\text{NLO}^\dagger/\text{NLO-EFT}$ and LO/LO-EFT.

Since NLO^* and NLO^\dagger only differ by their treatment of the finite virtual piece (c.f. eqs. (5) to (7)), we therefore focus on the difference in this piece only for now. Our results are presented in fig. 5 as a ratio of our NLO^* predictions to the NLO^\dagger one. For Higgs p_T less than $\simeq 225$ GeV the difference stays below 2%. Given that previously the rescaling employed by the NLO^\dagger prediction was an uncontrolled approximation, our new results validate this rescaling in the region of asymptotic series convergence.

We now turn our attention to the EFT rescaling options. For example in ref. [69] the LO/LO-EFT rescaling has been used to take into account top-mass effects at NNLO. With our improved NLO^* result we are able to justify this by studying the NLO rescaling $\text{NLO}^*/\text{NLO-EFT}$. We examine the various rescaling ratios in fig. 6 for the Higgs inclusive p_T spectrum.

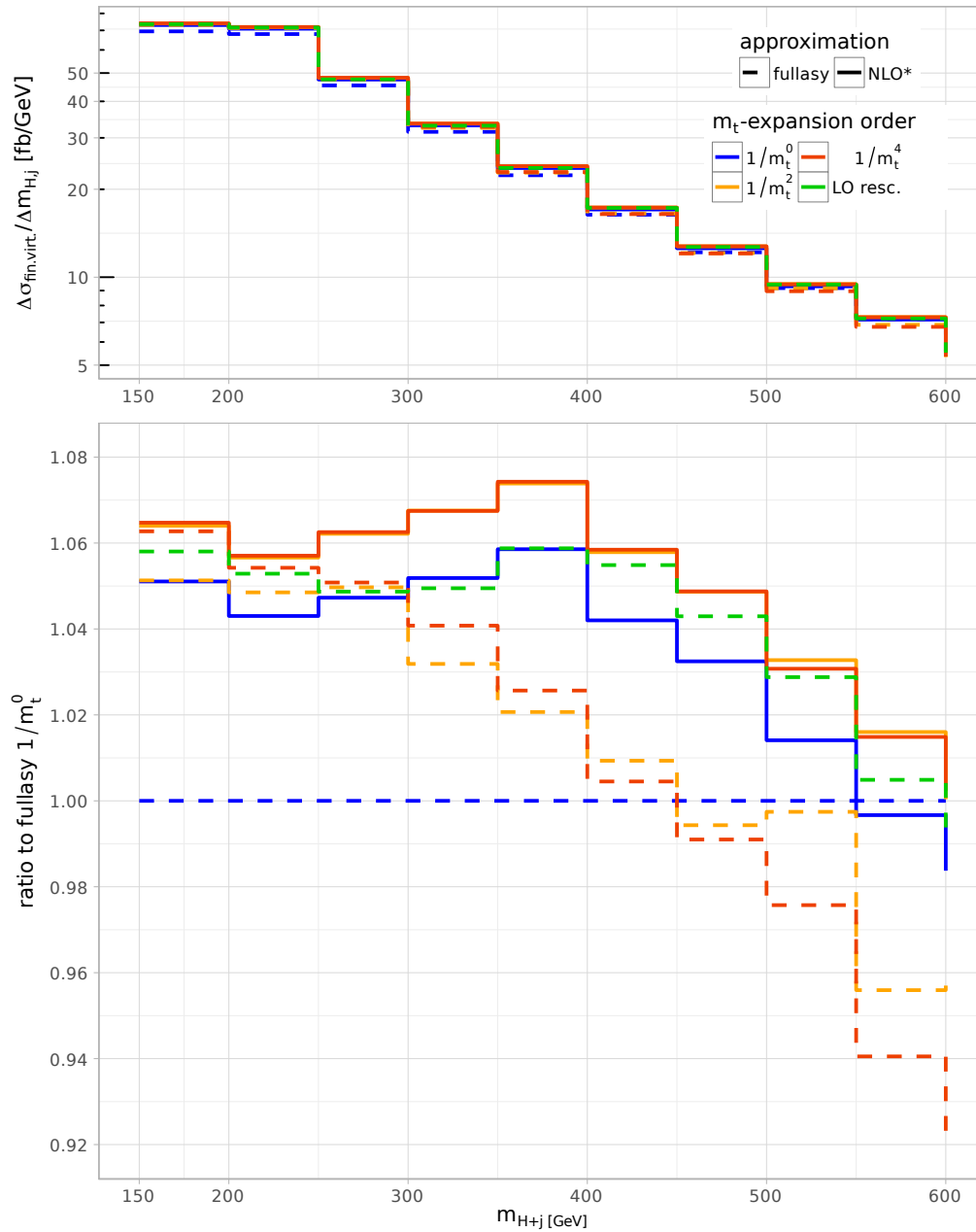


Figure 4: Invariant mass spectrum of the Higgs plus hardest jet system at NLO. The upper part displays the absolute distribution, while the lower part displays the ratio to the EFT result.

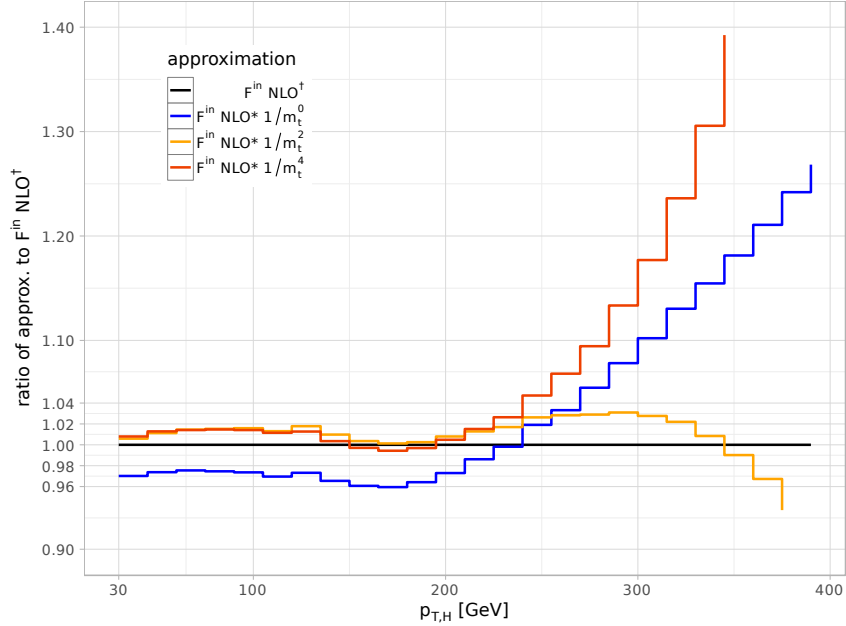


Figure 5: Ratio of the NLO* finite virtual piece $\mathcal{F}_{\text{SI}}^{\text{in}}$ in the asymptotic expansion as in eq. (7) to the LO rescaled EFT virtual piece $\mathcal{F}^{\text{in}} \text{NLO}^{\dagger}$ as in eq. (5).

In the upper panel the ratios are shown directly, whereas in the lower panel the ratio of the NLO* and NLO[†] rescaling ratios to the LO rescaling ratio are given. Any deviation from one indicates an error by just using the LO rescaling method to include top-mass effects. Up to $\simeq 225$ GeV the asymptotic series converges well and the ratios differ by less than three percent. Beyond 250 GeV the series clearly begins to diverge.

Note that although at 300 GeV the dependence on the asymptotic series reaches a few percent, the overall trend is to provide a somewhat larger rescaling ratio than the LO prediction. At 300 GeV an increase of at least 3-4% is indicated, being comparable to the NNLO scale uncertainty of $\simeq 8\%$ [69, 32, 29]. This is in agreement with the NLO[†] approach, which also suggests a reweighting leading to a harder p_T spectrum.

Our recommendation is to take into account the $\mathcal{O}(m_t^{-2})$ terms for our NLO* prediction. They capture the finite top-mass effects for low to medium p_T where the asymptotic series converges, and mimic the NLO[†] approximation toward higher p_T . This will be the default setting for the upcoming MCFM release that includes Higgs+jet at NLO* accuracy.

To consider a case where a LO rescaling is not possible smoothly, we now study the Higgs p_T distribution with an additional minimum jet transverse momentum requirement $p_{T,\text{jet}}^{\text{min}}$ in fig. 7. Each column of the plot shows a different jet cut $p_{T,\text{jet}}^{\text{min}}$ of 30,70 and 110 GeV,

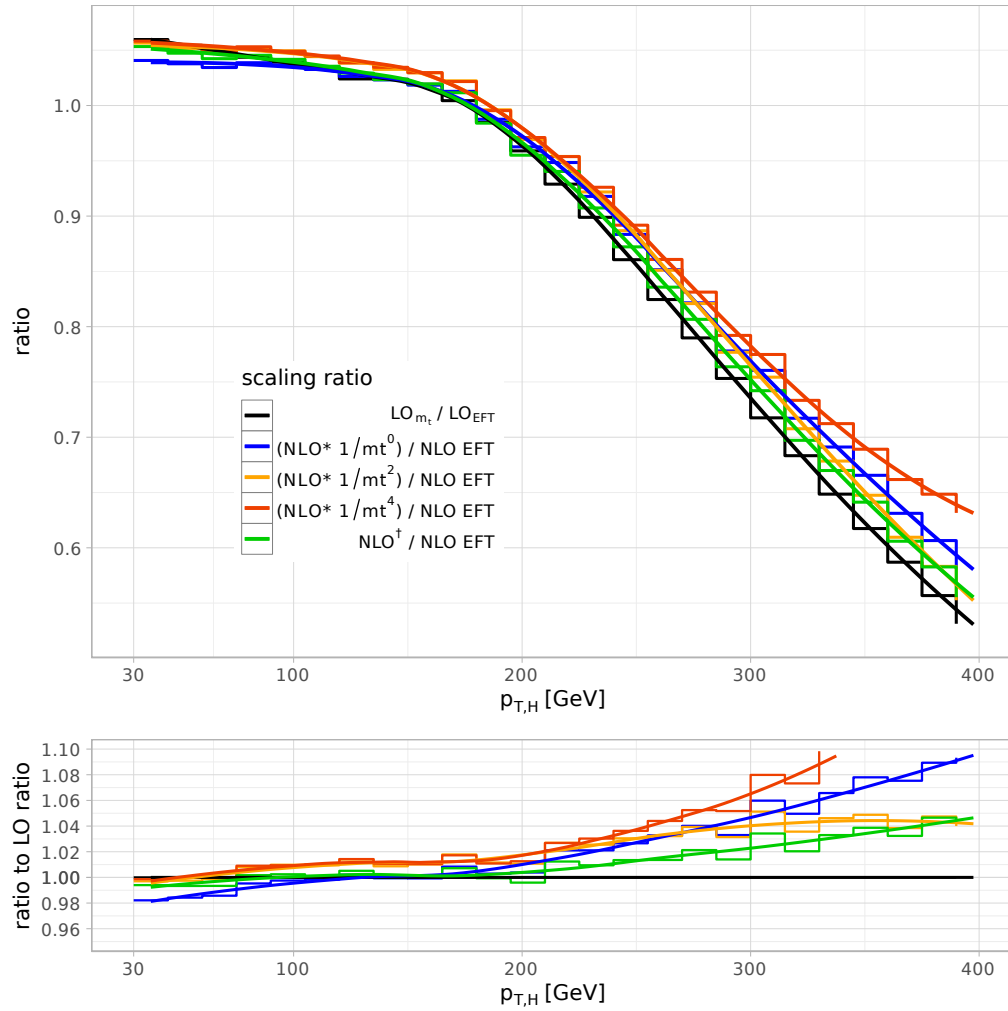


Figure 6: Rescaling ratios for the inclusion of mass effects in the NNLO Higgs inclusive p_T spectrum. The upper panel shows ratios directly, while the lower panel displays the ratio to the LO ratio to give an estimation of the error made by using the LO rescaling scheme. The solid lines are locally weighted scatterplot smoothing curves to guide the eye.

respectively. For comparison the NLO[†] approach is included again. Additionally, the LO rescaled full EFT result is included in purple. Note that for Higgs p_T smaller than the minimum jet transverse momentum $p_{T,\text{jet}}^{\text{min}}$ this rescaling breaks down, or is rather ill defined. Comparing both rescaling approaches with the NLO* prediction, we observe that they underestimate the mass effects by a few percent at high p_T . For 400 GeV the two rescaling approaches differ already by 4%, being comparable in size to the NNLO scale uncertainty. Again we recommend using the $\mathcal{O}(m_t^{-2})$ terms for our NLO* prediction with the same reasoning as above.

Finally, to see how far our NLO* result can improve predictions for p_T inclusive observables we consider the Higgs rapidity distribution in fig. 8. Throughout the whole range of rapidities the higher orders of the asymptotic expansion coincide within 0.5%. For large rapidities they coincide within the numerical uncertainty. Comparing this with the approach of LO rescaled virtual corrections NLO[†], we observe a discrepancy of 0.5% to 1%.

3.4 Higgs+jet NLO* phenomenology

In the previous subsection we have shown different approximations for Higgs+jet observables which take into account top-mass effects and discussed their limitations. We argued taking the $\mathcal{O}(m_t^{-2})$ mass corrections into account for our NLO* approximation as to get finite top-mass predictions up to scales of $\simeq 250$ GeV and reasonable predictions mimicking the rescaling behavior at higher energies. At energies above 300 GeV the remaining dependence on the asymptotic series becomes comparable in size to the residual NNLO scale uncertainty of $\simeq 8\%$ [69, 32, 29].

To estimate the dependence on the perturbative higher order corrections for the Higgs inclusive p_T distribution we show the variation of the factorization and renormalization scale $\mu_F = \mu_R = \mu = \sqrt{p_{T,H}^2 + m_H^2}$ by a factor of 2 and 1/2 in fig. 9. The change of the central value by $\simeq 20\%$ for the NLO* cross section and $\simeq 35\%$ for the LO cross section confirms earlier results [84]. Similarly, we show the scale variation results for the Higgs rapidity distribution in fig. 10. To obtain the best prediction for $H + \text{jet}$ observables we recommend taking the NNLO EFT results [69, 32, 29] and rescaling them by our NLO*/NLO-EFT K -factor to minimize the scale dependence *and* top-mass uncertainty.

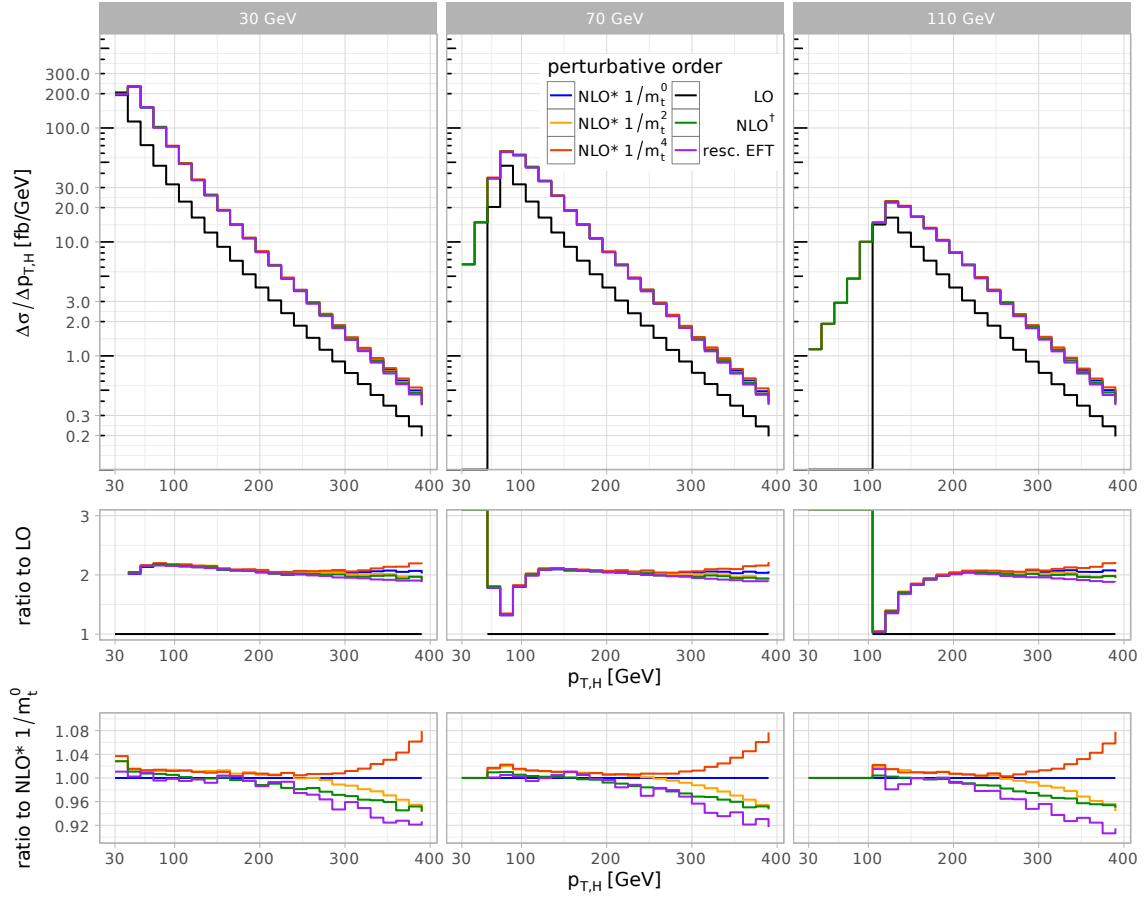


Figure 7: NLO* transverse momentum distributions of the Higgs boson with minimum jet transverse momenta of 30, 70 and 110 GeV. The upper panel shows the absolute distribution, while the lower two panels display the ratio to the LO distribution and the NLO* $1/m_t^0$ approximation, respectively.

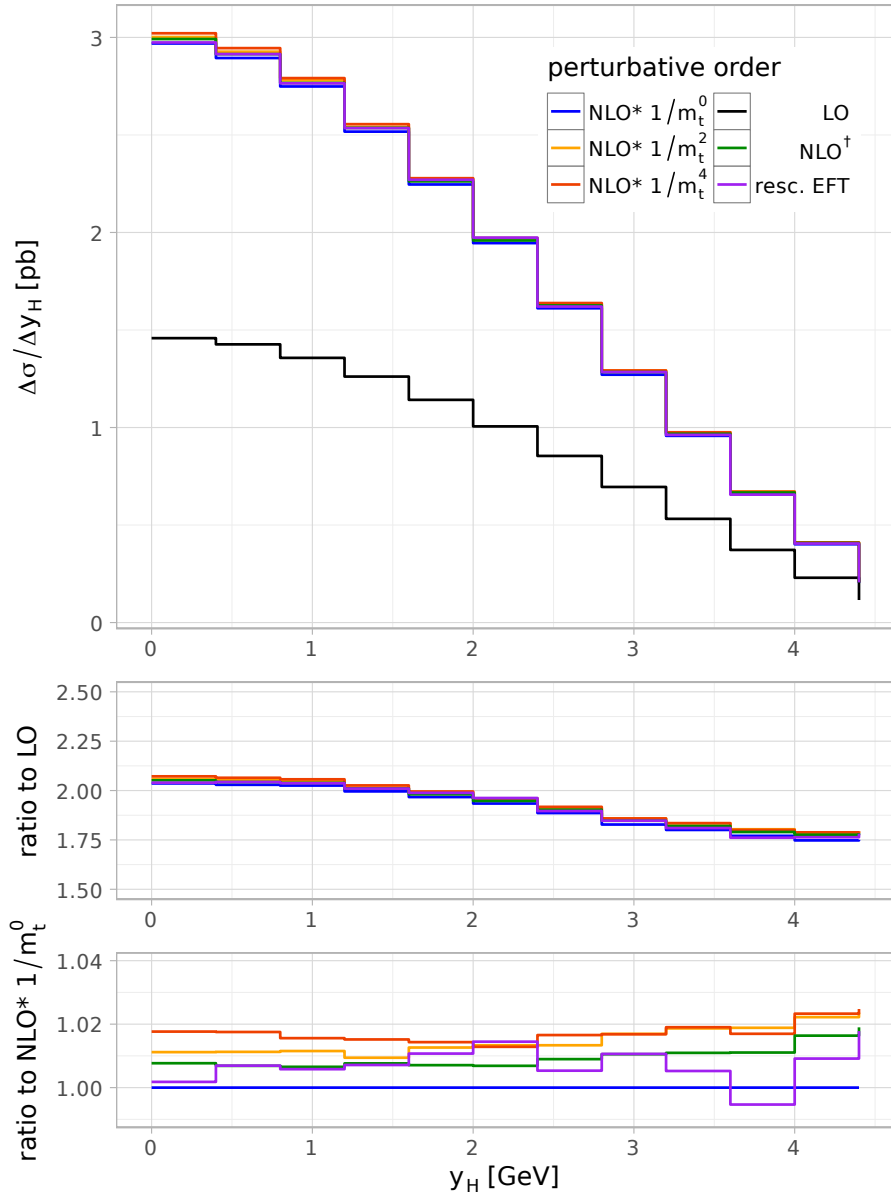


Figure 8: Higgs rapidity distribution for different orders and approximations. The upper panel shows the absolute distribution, while the lower two panels display the ratio to the LO distribution and the $\text{NLO}^* 1/m_t^0$ approximation, respectively.

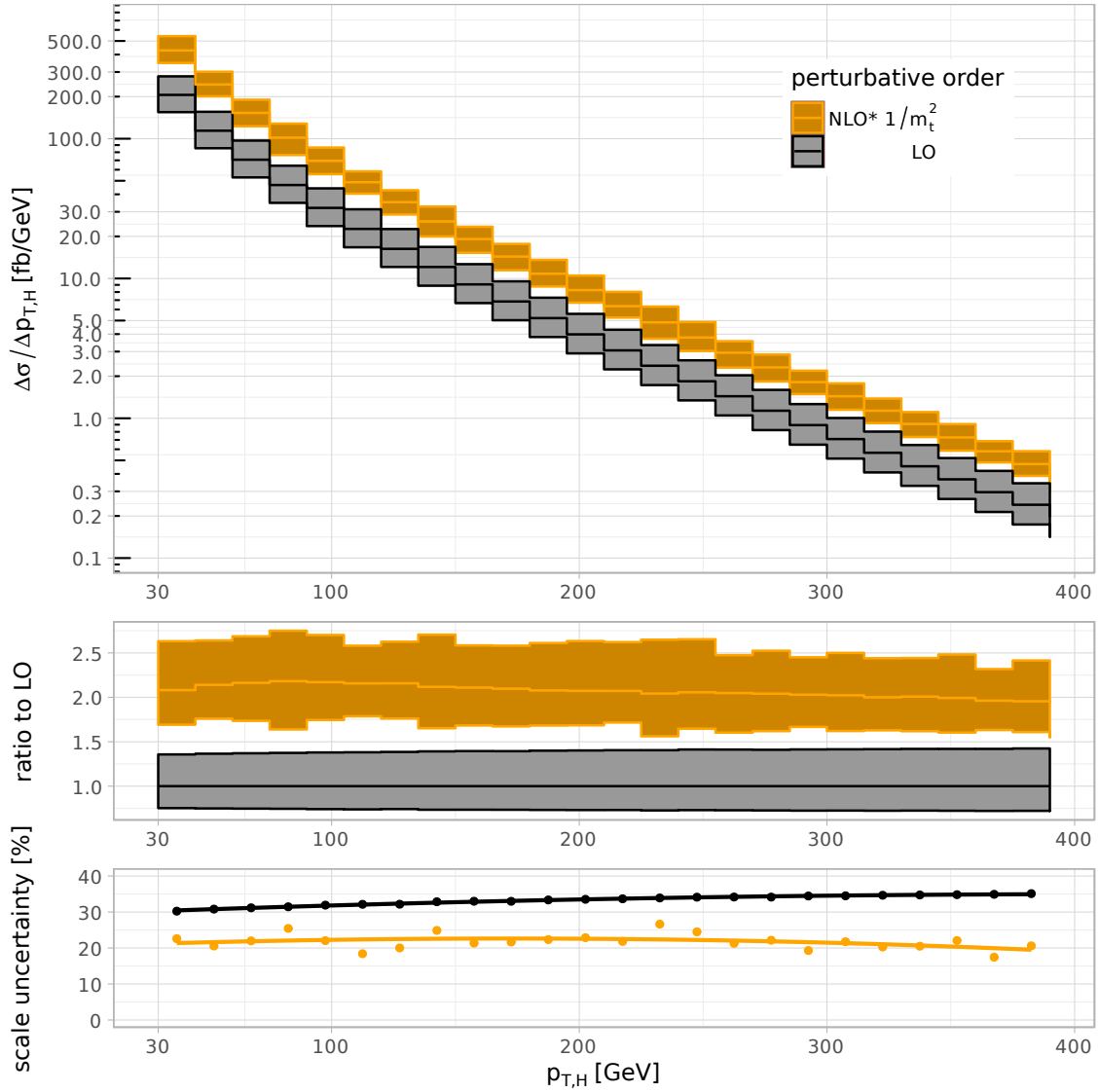


Figure 9: Higgs inclusive transverse momentum distribution at LO and NLO*. The ribbon is obtained by varying the factorization and renormalization scale $\mu = \sqrt{p_{T,H}^2 + m_H^2}$ by a factor of 2 and 1/2. The middle panel shows the ratio to the LO cross section. The lower panel shows the mean of the upper and lower bound change with respect to the central value in percent, commonly known as the scale uncertainty.

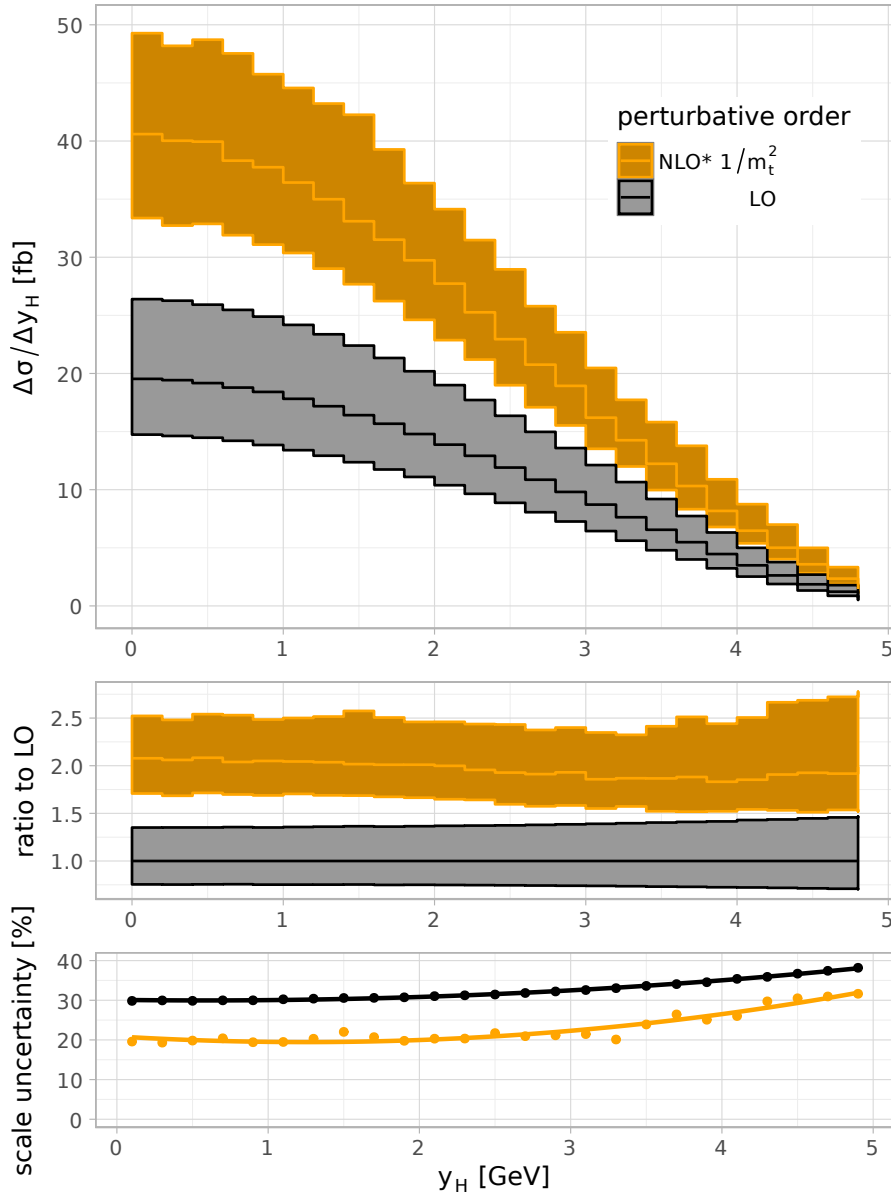


Figure 10: Higgs rapidity distribution at LO and NLO*. The ribbon is obtained by varying the factorization and renormalization scale $\mu = \sqrt{p_{T,H}^2 + m_H^2}$ by a factor of 2 and 1/2. The middle panel shows the ratio to the LO cross section. The lower panel shows the mean of the upper and lower bound change with respect to the central value in percent, commonly known as the scale uncertainty.

4 Conclusions

We presented a calculation of H+jet production at NLO accuracy with full top-mass dependence in all components as far as possible with current technology: only the finite part of two-loop amplitude entering the virtual corrections is taken in an asymptotic expansion in Λ/m_t , where Λ can be any kinematical scale of the process. The convergence of the asymptotic expansion allowed us to predict the full top-mass dependence for transverse momenta smaller than $\simeq 225$ GeV and quantify a remaining uncertainty for higher energies.

Previous approaches to include top-mass effects for H+jet cross sections were, for example, to rescale the EFT result by the ratio of the m_t -exact to the EFT cross section at LO. From a different point of view this equates to using the EFT K -factor for the m_t -exact LO. Further approximations have been made, taking the two parton real emission m_t -exactly into account and LO rescaling the fully EFT virtual corrections.

We validated the use of these LO rescaling schemes to a few percent for Higgs p_T distributions up to $\simeq 250$ GeV and provide m_t exact predictions using the higher order corrections $1/m_t^2, 1/m_t^4$ for scales up to $\simeq 225$ GeV. For energies larger than $\simeq 300$ GeV the estimated error made by using the LO rescaling scheme becomes comparable in size to the NNLO scale uncertainty of $\simeq 8\%$ and a full calculation of the two-loop integrals is advised. We recommend using our NLO* $\mathcal{O}(1/m_t^2)$ corrections to make predictions over the full kinematical range: We believe they are very close to the m_t -exact results for $p_T \lesssim 225$ GeV and mimic the LO rescaled virtual corrections scheme for larger p_T . Alternatively one could consider a combination with the m_t -exact high p_T limit in ref. [58]. For sufficiently exclusive cuts, where no mapping to a born phase space is possible, an NLO rescaling, using for example our NLO* result, is needed.

To conclude, our NLO* approximation for Higgs+jet production gives top-mass improved results up to high kinematical scales of $\simeq 300$ GeV relevant for LHC Run II by including m_t -exact parts as far as currently possible and by exploiting asymptotic expansions for the remaining two-loop integrals. Our work facilitates the construction of the best fixed order Higgs+jet observables, by rescaling the NNLO-EFT results with our NLO*/NLO-EFT top-mass corrections K -factor.

Acknowledgments We are grateful to Stefano Carrazza for providing us with an advanced copy of QCDLoop 2.0. We would like to thank Tom Zirke for help with the exp/q2e-setup and Robert Harlander and Frank Petriello for useful comments. Support was provided by the Center for Computational Research at the University at Buffalo. CW is supported by the National Science Foundation through award number PHY-1619877.

References

- [1] **CMS** Collaboration, S. Chatrchyan et al., *Observation of a new boson at a mass of 125 GeV with the CMS experiment at the LHC*, *Phys. Lett.* **B716** (2012) 30–61, [arXiv:1207.7235].
- [2] **ATLAS** Collaboration, G. Aad et al., *Observation of a new particle in the search for the Standard Model Higgs boson with the ATLAS detector at the LHC*, *Phys. Lett.* **B716** (2012) 1–29, [arXiv:1207.7214].
- [3] **ATLAS** Collaboration, G. Aad et al., *Measurements of the Total and Differential Higgs Boson Production Cross Sections Combining the $H \rightarrow \gamma\gamma$ and $H \rightarrow ZZ^* \rightarrow 4\ell$ Decay Channels at $\sqrt{s} = 8$ TeV with the ATLAS Detector*, *Phys. Rev. Lett.* **115** (2015), no. 9 091801, [arXiv:1504.0583].
- [4] **ATLAS** Collaboration, T. A. collaboration, *Measurements of the Higgs boson production and decay rates and coupling strengths using pp collision data at $\sqrt{s} = 7$ and 8 TeV in the ATLAS experiment*, .
- [5] **ATLAS** Collaboration, G. Aad et al., *Study of the spin and parity of the Higgs boson in diboson decays with the ATLAS detector*, *Eur. Phys. J.* **C75** (2015), no. 10 476, [arXiv:1506.0566]. [Erratum: *Eur. Phys. J.*C76,no.3,152(2016)].
- [6] **CMS** Collaboration, V. Khachatryan et al., *Precise determination of the mass of the Higgs boson and tests of compatibility of its couplings with the standard model predictions using proton collisions at 7 and 8 TeV*, *Eur. Phys. J.* **C75** (2015), no. 5 212, [arXiv:1412.8662].
- [7] **ATLAS** Collaboration, G. Aad et al., *Measurements of the Higgs boson production and decay rates and coupling strengths using pp collision data at $\sqrt{s} = 7$ and 8 TeV in the ATLAS experiment*, *Eur. Phys. J.* **C76** (2016), no. 1 6, [arXiv:1507.0454].
- [8] P. P. Giardino, K. Kannike, I. Masina, M. Raidal, and A. Strumia, *The universal Higgs fit*, *JHEP* **05** (2014) 046, [arXiv:1303.3570].
- [9] C. Anastasiou, C. Duhr, F. Dulat, F. Herzog, and B. Mistlberger, *Higgs Boson Gluon-Fusion Production in QCD at Three Loops*, *Phys. Rev. Lett.* **114** (2015) 212001, [arXiv:1503.0605].
- [10] C. Anastasiou, C. Duhr, F. Dulat, E. Furlan, T. Gehrmann, F. Herzog, A. Lazopoulos, and B. Mistlberger, *High precision determination of the gluon fusion Higgs boson cross-section at the LHC*, *JHEP* **05** (2016) 058, [arXiv:1602.0069].
- [11] **ATLAS** Collaboration, G. Aad et al., *Measurement of fiducial differential cross sections of*

gluon-fusion production of Higgs bosons decaying to $WW^ \rightarrow e\nu\mu\nu$ with the ATLAS detector at $\sqrt{s} = 8$ TeV*, arXiv:1604.0299.

- [12] **ATLAS** Collaboration, G. Aad et al., *Constraints on non-Standard Model Higgs boson interactions in an effective Lagrangian using differential cross sections measured in the $H \rightarrow \gamma\gamma$ decay channel at $\sqrt{s} = 8$ TeV with the ATLAS detector*, *Phys. Lett.* **B753** (2016) 69–85, [arXiv:1508.0250].
- [13] **ATLAS** Collaboration, G. Aad et al., *Fiducial and differential cross sections of Higgs boson production measured in the four-lepton decay channel in pp collisions at $\sqrt{s}=8$ TeV with the ATLAS detector*, *Phys. Lett.* **B738** (2014) 234–253, [arXiv:1408.3226].
- [14] **ATLAS** Collaboration, G. Aad et al., *Measurements of fiducial and differential cross sections for Higgs boson production in the diphoton decay channel at $\sqrt{s} = 8$ TeV with ATLAS*, *JHEP* **09** (2014) 112, [arXiv:1407.4222].
- [15] **CMS** Collaboration, V. Khachatryan et al., *Measurement of differential and integrated fiducial cross sections for Higgs boson production in the four-lepton decay channel in pp collisions at $\sqrt{s} = 7$ and 8 TeV*, *JHEP* **04** (2016) 005, [arXiv:1512.0837].
- [16] **CMS** Collaboration, V. Khachatryan et al., *Measurement of differential cross sections for Higgs boson production in the diphoton decay channel in pp collisions at $\sqrt{s} = 8$ TeV*, *Eur. Phys. J.* **C76** (2016), no. 1 13, [arXiv:1508.0781].
- [17] **CMS** Collaboration, V. Khachatryan et al., *Measurement of the transverse momentum spectrum of the Higgs boson produced in pp collisions at $\sqrt{s} = 8$ TeV using the $H \rightarrow WW$ decays*, .
- [18] R. V. Harlander and T. Neumann, *Probing the nature of the Higgs-gluon coupling*, *Phys. Rev.* **D88** (2013) 074015, [arXiv:1308.2225].
- [19] S. Dawson, I. M. Lewis, and M. Zeng, *Effective field theory for Higgs boson plus jet production*, *Phys. Rev.* **D90** (2014), no. 9 093007, [arXiv:1409.6299].
- [20] S. Dawson, I. M. Lewis, and M. Zeng, *Usefulness of effective field theory for boosted Higgs production*, *Phys. Rev.* **D91** (2015) 074012, [arXiv:1501.0410].
- [21] A. Banfi, A. Martin, and V. Sanz, *Probing top-partners in Higgs+jets*, *JHEP* **08** (2014) 053, [arXiv:1308.4771].
- [22] A. Azatov and A. Paul, *Probing Higgs couplings with high p_T Higgs production*, *JHEP* **01** (2014) 014, [arXiv:1309.5273].
- [23] C. Grojean, E. Salvioni, M. Schlaffer, and A. Weiler, *Very boosted Higgs in gluon fusion*, *JHEP* **05** (2014) 022, [arXiv:1312.3317].

- [24] M. Schlaffer, M. Spannowsky, M. Takeuchi, A. Weiler, and C. Wymant, *Boosted Higgs Shapes*, *Eur. Phys. J.* **C74** (2014), no. 10 3120, [arXiv:1405.4295].
- [25] M. Buschmann, C. Englert, D. Goncalves, T. Plehn, and M. Spannowsky, *Resolving the Higgs-Gluon Coupling with Jets*, *Phys. Rev.* **D90** (2014), no. 1 013010, [arXiv:1405.7651].
- [26] M. Buschmann, D. Goncalves, S. Kuttimalai, M. Schönherr, F. Krauss, and T. Plehn, *Mass Effects in the Higgs-Gluon Coupling: Boosted vs Off-Shell Production*, *JHEP* **02** (2015) 038, [arXiv:1410.5806].
- [27] U. Langenegger, M. Spira, and I. Strebel, *Testing the Higgs Boson Coupling to Gluons*, arXiv:1507.0137.
- [28] D. Ghosh and M. Wiebusch, *Dimension-six triple gluon operator in Higgs+jet observables*, *Phys. Rev.* **D91** (2015), no. 3 031701, [arXiv:1411.2029].
- [29] R. Boughezal, F. Caola, K. Melnikov, F. Petriello, and M. Schulze, *Higgs boson production in association with a jet at next-to-next-to-leading order in perturbative QCD*, *JHEP* **06** (2013) 072, [arXiv:1302.6216].
- [30] X. Chen, T. Gehrmann, E. W. N. Glover, and M. Jaquier, *Precise QCD predictions for the production of Higgs + jet final states*, *Phys. Lett.* **B740** (2015) 147–150, [arXiv:1408.5325].
- [31] R. Boughezal, F. Caola, K. Melnikov, F. Petriello, and M. Schulze, *Higgs boson production in association with a jet at next-to-next-to-leading order*, *Phys. Rev. Lett.* **115** (2015), no. 8 082003, [arXiv:1504.0792].
- [32] R. Boughezal, C. Focke, W. Giele, X. Liu, and F. Petriello, *Higgs boson production in association with a jet at NNLO using jetiness subtraction*, *Phys. Lett.* **B748** (2015) 5–8, [arXiv:1505.0389].
- [33] J. M. Campbell, R. K. Ellis, and G. Zanderighi, *Next-to-Leading order Higgs + 2 jet production via gluon fusion*, *JHEP* **10** (2006) 028, [hep-ph/0608194].
- [34] J. M. Campbell, R. K. Ellis, and C. Williams, *Hadronic production of a Higgs boson and two jets at next-to-leading order*, *Phys. Rev.* **D81** (2010) 074023, [arXiv:1001.4495].
- [35] G. Cullen, H. van Deurzen, N. Greiner, G. Luisoni, P. Mastrolia, E. Mirabella, G. Ossola, T. Peraro, and F. Tramontano, *Next-to-Leading-Order QCD Corrections to Higgs Boson Production Plus Three Jets in Gluon Fusion*, *Phys. Rev. Lett.* **111** (2013), no. 13 131801, [arXiv:1307.4737].
- [36] D. Graudenz, M. Spira, and P. M. Zerwas, *QCD corrections to Higgs boson production at proton proton colliders*, *Phys. Rev. Lett.* **70** (1993) 1372–1375.

- [37] R. Harlander and P. Kant, *Higgs production and decay: Analytic results at next-to-leading order QCD*, *JHEP* **12** (2005) 015, [[hep-ph/0509189](#)].
- [38] C. Anastasiou, S. Beerli, S. Bucherer, A. Daleo, and Z. Kunszt, *Two-loop amplitudes and master integrals for the production of a Higgs boson via a massive quark and a scalar-quark loop*, *JHEP* **01** (2007) 082, [[hep-ph/0611236](#)].
- [39] R. V. Harlander and K. J. Ozeren, *Finite top mass effects for hadronic Higgs production at next-to-next-to-leading order*, *JHEP* **11** (2009) 088, [[arXiv:0909.3420](#)].
- [40] A. Pak, M. Rogal, and M. Steinhauser, *Finite top quark mass effects in NNLO Higgs boson production at LHC*, *JHEP* **02** (2010) 025, [[arXiv:0911.4662](#)].
- [41] R. V. Harlander and K. J. Ozeren, *Top mass effects in Higgs production at next-to-next-to-leading order QCD: Virtual corrections*, *Phys. Lett.* **B679** (2009) 467–472, [[arXiv:0907.2997](#)].
- [42] A. Pak, M. Rogal, and M. Steinhauser, *Virtual three-loop corrections to Higgs boson production in gluon fusion for finite top quark mass*, *Phys. Lett.* **B679** (2009) 473–477, [[arXiv:0907.2998](#)].
- [43] R. V. Harlander, S. Liebler, and H. Mantler, *SusHi Bento: Beyond NNLO and the heavy-top limit*, [arXiv:1605.0319](#).
- [44] S. Marzani, R. D. Ball, V. Del Duca, S. Forte, and A. Vicini, *Finite-top-mass effects in NNLO Higgs production*, *Nucl. Phys. Proc. Suppl.* **186** (2009) 98–101, [[arXiv:0809.4934](#)].
- [45] S. Marzani, R. D. Ball, V. Del Duca, S. Forte, and A. Vicini, *Higgs production via gluon-gluon fusion with finite top mass beyond next-to-leading order*, *Nucl. Phys.* **B800** (2008) 127–145, [[arXiv:0801.2544](#)].
- [46] R. V. Harlander, H. Mantler, S. Marzani, and K. J. Ozeren, *Higgs production in gluon fusion at next-to-next-to-leading order QCD for finite top mass*, *Eur. Phys. J.* **C66** (2010) 359–372, [[arXiv:0912.2104](#)].
- [47] V. Del Duca, W. Kilgore, C. Oleari, C. R. Schmidt, and D. Zeppenfeld, *Kinematical limits on Higgs boson production via gluon fusion in association with jets*, *Phys. Rev.* **D67** (2003) 073003, [[hep-ph/0301013](#)].
- [48] U. Baur and E. W. N. Glover, *Higgs Boson Production at Large Transverse Momentum in Hadronic Collisions*, *Nucl. Phys.* **B339** (1990) 38–66.
- [49] R. K. Ellis, I. Hinchliffe, M. Soldate, and J. J. van der Bij, *Higgs Decay to $\tau^+ \tau^-$: A Possible Signature of Intermediate Mass Higgs Bosons at the SSC*, *Nucl. Phys.* **B297** (1988) 221–243.

- [50] V. Del Duca, W. Kilgore, C. Oleari, C. Schmidt, and D. Zeppenfeld, *Higgs + 2 jets via gluon fusion*, *Phys. Rev. Lett.* **87** (2001) 122001, [hep-ph/0105129].
- [51] V. Del Duca, W. Kilgore, C. Oleari, C. Schmidt, and D. Zeppenfeld, *Gluon fusion contributions to H + 2 jet production*, *Nucl. Phys.* **B616** (2001) 367–399, [hep-ph/0108030].
- [52] F. Campanario and M. Kubocz, *Higgs boson production in association with three jets via gluon fusion at the LHC: Gluonic contributions*, *Phys. Rev.* **D88** (2013), no. 5 054021, [arXiv:1306.1830].
- [53] N. Greiner, S. Hoeche, G. Luisoni, M. Schönherr, and J.-C. Winter, *Full mass dependence in Higgs boson production in association with jets at the LHC and FCC*, arXiv:1608.0119.
- [54] R. Frederix, S. Frixione, E. Vryonidou, and M. Wiesemann, *Heavy-quark mass effects in Higgs plus jets production*, arXiv:1604.0301.
- [55] S. Borowka, N. Greiner, G. Heinrich, S. P. Jones, M. Kerner, J. Schlenk, and T. Zirke, *Full top quark mass dependence in Higgs boson pair production at NLO*, arXiv:1608.0479.
- [56] S. Borowka, N. Greiner, G. Heinrich, S. Jones, M. Kerner, J. Schlenk, U. Schubert, and T. Zirke, *Higgs Boson Pair Production in Gluon Fusion at Next-to-Leading Order with Full Top-Quark Mass Dependence*, *Phys. Rev. Lett.* **117** (2016), no. 1 012001, [arXiv:1604.0644]. [Erratum: *Phys. Rev. Lett.* 117, no. 7, 079901 (2016)].
- [57] S. Forte and C. Muselli, *High energy resummation of transverse momentum distributions: Higgs in gluon fusion*, *JHEP* **03** (2016) 122, [arXiv:1511.0556].
- [58] F. Caola, S. Forte, S. Marzani, C. Muselli, and G. Vita, *The Higgs transverse momentum spectrum with finite quark masses beyond leading order*, arXiv:1606.0410.
- [59] T. Neumann and M. Wiesemann, *Finite top-mass effects in gluon-induced Higgs production with a jet-veto at NNLO*, *JHEP* **1411** (2014) 150, [arXiv:1408.6836].
- [60] R. V. Harlander, T. Neumann, K. J. Ozeren, and M. Wiesemann, *Top-mass effects in differential Higgs production through gluon fusion at order α_s^4* , *JHEP* **1208** (2012) 139, [arXiv:1206.0157].
- [61] J. M. Campbell and R. K. Ellis, *An Update on vector boson pair production at hadron colliders*, *Phys. Rev.* **D60** (1999) 113006, [hep-ph/9905386].
- [62] J. M. Campbell, R. K. Ellis, and C. Williams, *Vector boson pair production at the LHC*, *JHEP* **07** (2011) 018, [arXiv:1105.0020].

- [63] J. M. Campbell, R. K. Ellis, and W. T. Giele, *A Multi-Threaded Version of MCFM*, *Eur. Phys. J.* **C75** (2015), no. 6 246, [arXiv:1503.0618].
- [64] H. Mantler, *Bottom-Quark-Effekte in der Higgs-Produktion*, Master's thesis, University of Wuppertal, 2009.
- [65] W.-Y. Keung and F. J. Petriello, *Electroweak and finite quark-mass effects on the Higgs boson transverse momentum distribution*, *Phys. Rev.* **D80** (2009) 013007, [arXiv:0905.2775].
- [66] R. V. Harlander, S. Liebler, and H. Mantler, *SusHi: A program for the calculation of Higgs production in gluon fusion and bottom-quark annihilation in the Standard Model and the MSSM*, *Comput. Phys. Commun.* **184** (2013) 1605–1617, [arXiv:1212.3249].
- [67] R. Bonciani, V. Del Duca, H. Frellesvig, J. M. Henn, F. Moriello, and V. A. Smirnov, *Next-to-leading order QCD corrections to the decay width $H \rightarrow Z\gamma$* , *JHEP* **08** (2015) 108, [arXiv:1505.0056].
- [68] S. Catani and M. H. Seymour, *A General algorithm for calculating jet cross-sections in NLO QCD*, *Nucl. Phys.* **B485** (1997) 291–419, [hep-ph/9605323]. [Erratum: *Nucl. Phys.*B510,503(1998)].
- [69] X. Chen, J. Cruz-Martinez, T. Gehrmann, E. W. N. Glover, and M. Jaquier, *NNLO QCD corrections to Higgs boson production at large transverse momentum*, arXiv:1607.0881.
- [70] R. Harlander, *Asymptotic expansions: Methods and applications*, *Acta Phys. Polon.* **B30** (1999) 3443–3462, [hep-ph/9910496].
- [71] V. A. Smirnov, *Applied asymptotic expansions in momenta and masses*, *Springer Tracts Mod. Phys.* **177** (2002) 1–262.
- [72] S. D. Badger, *Direct Extraction Of One Loop Rational Terms*, *JHEP* **01** (2009) 049, [arXiv:0806.4600].
- [73] P. Mastrolia, *Double-Cut of Scattering Amplitudes and Stokes' Theorem*, *Phys. Lett.* **B678** (2009) 246–249, [arXiv:0905.2909].
- [74] D. Maître and P. Mastrolia, *S@M, a Mathematica Implementation of the Spinor-Helicity Formalism*, *Comput. Phys. Commun.* **179** (2008) 501–574, [arXiv:0710.5559].
- [75] R. K. Ellis, W. T. Giele, Z. Kunszt, and K. Melnikov, *Masses, fermions and generalized D-dimensional unitarity*, *Nucl. Phys.* **B822** (2009) 270–282, [arXiv:0806.3467].
- [76] V. A. Smirnov, *Asymptotic expansions in momenta and masses and calculation of Feynman diagrams*, *Mod. Phys. Lett.* **A10** (1995) 1485–1500, [hep-th/9412063].

- [77] R. Harlander, T. Seidensticker, and M. Steinhauser, *Corrections of $\mathcal{O}(\alpha\alpha_s)$ to the decay of the Z boson into bottom quarks*, *Phys. Lett.* **B426** (1998) 125–132, [hep-ph/9712228].
- [78] T. Seidensticker, *Automatic application of successive asymptotic expansions of Feynman diagrams*, hep-ph/9905298.
- [79] M. Steinhauser, *MATAD: A Program package for the computation of MAssive TADpoles*, *Comput. Phys. Commun.* **134** (2001) 335–364, [hep-ph/0009029].
- [80] A. von Manteuffel and C. Studerus, *Reduze 2 - Distributed Feynman Integral Reduction*, arXiv:1201.4330.
- [81] R. K. Ellis and G. Zanderighi, *Scalar one-loop integrals for QCD*, *JHEP* **02** (2008) 002, [arXiv:0712.1851].
- [82] S. Carrazza, R. K. Ellis, and G. Zanderighi, *QCDLoop: a comprehensive framework for one-loop scalar integrals*, arXiv:1605.0318.
- [83] S. Dulat, T.-J. Hou, J. Gao, M. Guzzi, J. Huston, P. Nadolsky, J. Pumplin, C. Schmidt, D. Stump, and C. P. Yuan, *New parton distribution functions from a global analysis of quantum chromodynamics*, *Phys. Rev.* **D93** (2016), no. 3 033006, [arXiv:1506.0744].
- [84] D. de Florian, M. Grazzini, and Z. Kunszt, *Higgs production with large transverse momentum in hadronic collisions at next-to-leading order*, *Phys. Rev. Lett.* **82** (1999) 5209–5212, [hep-ph/9902483].